Bioinspired Polymeric Coating with Self-Adhesion, Lubrication, and Drug Release for Synergistic Bacteriostatic and Bactericidal Performance

Haimang Wang[a], Yuhe Yang[b,c], Weiwei Zhao[a], Ying Han[a], Jing Luo[d], Xin Zhao[b,c], Hongyu Zhang[a]

[a] *State Key Laboratory of Tribology, Department of Mechanical Engineering, Tsinghua University, Beijing, 100084, China*

[b] *Department of Biomedical Engineering, The Hong Kong Polytechnic University, Hung Hom, Hong Kong SAR, China.*

[c] *The Hong Kong Polytechnic University Shenzhen Research InstituteShenzhen 518000, China*

[d] *Beijing Research Institute of Automation for Machinery Industry Co., LtdBeijing 100120, China*

ABSTRACT: A combination of surface lubrication and antibacterial performance is highly imperative for biomedical implants in clinic. In this study, motivated by mussel-inspired adhesion, articular cartilage superlubrication, and drug-loading capacity of cyclodextrins, a new copolymer of p(DMA-MPC-CD) (namely PDMC) with self-adhesion, lubrication, and drug loading & release properties is developed for fabricating a versatile platform to construct a synergistic bacteriostatic/bactericidal surface. Specifically, the biomimetic coating is prepared via polydopamine mediated layer-by-layer (LBL) self-assembly method on the surface of titanium alloy (Ti6Al4V), and characterized by quartz crystal microbalance, X-ray photoelectron spectroscopy, and

surface wettability to confirm the modification process. The biocompatibility evaluation using L929 cells shows that the coating, even with pre-loaded bactericide, presents satisfied biocompatibility in vitro. Additionally, the enhanced lubrication and bacterial resistance properties of copolymer-coated Ti6Al4V (Ti6Al4V@PDMC) are attributed to the tenacious hydration shell that is formed surrounding the zwitterionic phosphorylcholine charges. Furthermore, the bactericidal function of the biomimetic coating is successfully achieved by releasing the pre-loaded bactericide in a sustained manner, which effectively kills the adhered bacteria on the surface. In summary, the bioinspired surface functionalization strategy developed here may act as a universal and promising method for achieving enhanced lubrication and synergistic bacteriostatic/bactericidal properties in biomedical implants.

1. Introduction

Advanced interventional biomedical implants have been widely used in clinic with a great demand in recent years. However, limited surface lubrication and bacterial biofilm formation, which can induce severe soft tissue damage and correspondingly a series of consecutive complications, are regarded to be two important challenges associated with the biomedical implants, but up to now, no effective approaches have been developed to address this issue.[1-3] To function properly, complex surface modifications are often required for the implants to reduce interfacial friction and bacterial infection. Nowadays, natural systems become a great source of inspiration for material scientists in designing lubricated or antibacterial surface of biomedical implants. For instance, the lubrication coatings based on various biomacromolecules in articular cartilage (e.g.,

hyaluronan,[4] mucin,[5] and phospholipids[6]), and antibacterial coatings based on natural bactericidal substances produced by living organisms (e.g., antimicrobial peptides,[7] bacteriolytic enzymes,[8] and essential oils[9]) or natural antimicrobial surface of animal organ (e.g., cicada wing[10] and gecko skin[11]), have been comprehensively reported in the field of biomedical engineering. However, despite the rapid development of different lubricated or antibacterial coatings, relatively few studies have been performed to simultaneously combine lubrication and antibacterial properties for achieving surface functionalization of biomedical implant. A synergistic design with enhanced lubrication and antibacterial mechanism represents a prospective approach to overcome the intrinsic limitations of each strategy. Accordingly, it is particularly meaningful to develop a versatile platform for constructing a lubricated and antibacterial surface for biomedical implants.

In nature, healthy articular cartilage has excellent superlubrication property even under high physiological loadings based on the hydration lubrication mechanism. The friction coefficient (COF), measured utilizing a surface force balance, is extremely low with a value of less than 0.001, and it is attributed to the supramolecular synergy of the charged brush-like biomacromolecules.[12] Klein et al. have shown that the biomacromolecules containing phosphatidylcholine lipid can attract many water molecules through dipole-charge interaction and form a tenacious hydration shell around the zwitterionic charges, that is, $PO4^-$ and $N^+(CH3)3$.[13, 14] The hydration shell behaves in a fluid-like manner under shear and significantly reduces interfacial COF between two sliding surfaces. Inspired by articular cartilage superlubrication, a

variety of zwitterionic polymers, for example, poly(2-methacryloyloxyethyl phosphorylcholine) (PMPC),[15, 16] and poly(sulfobetaine methacrylate) (PSBMA),[17] have been developed to enhance lubrication performance of biomaterial surfaces with favorable hydrophilicity and biocompatibility. However, the complicated surface modification procedure and instability of the lubricated coating greatly limit their clinical applications. In addition, many studies on bacterial infection of biomedical implants have indicated that a reversible initial bacterial adhesion is the first step, which is followed by the transition to an enhanced irreversible adhesion and finally develops into a mature biofilm.[18] To achieve antibacterial surfaces, zwitterionic polymeric coatings using the hydration shell to resist bacterial adhesion have also been investigated.[19, 20] However, it should be noted that these zwitterionic polymers cannot completely prevent bacterial adhesion and kill the adhered bacteria, which is important to inhibit the formation of bacterial biofilms.[21]

Therefore, a universal and facile surface modification technique that can functionalize the substrate with effective lubrication and antibacterial properties is imperative. In our previous studies,[15, 16] motivated by the mussel-inspired adhesion and articular cartilage superlubrication,[22] a self-adhesive copolymer, that is, p(DMA-MPC), has been reported. This coating, is synthesized based on dopamine methacrylamide (DMA) and 2-methacryloyloxyethyl phosphorylcholine (MPC), and enhance lubrication and achieve bacterial resistance performance owing to hydration lubrication and hydration repulsive interactions. Here, we aim to endow the DMA-MPC copolymer with drug delivery property by the introduction of cyclodextrins (CDs),

which can encapsulate bactericide into the cavity and then release the preloaded molecules over a prolonged period of time, relying on the internal hydrophobic cavity and external hydrophilic surface.[23] Therefore, a new copolymer, that is, p(DMA-MPC-CD) with the property of self-adhesion, lubrication, and drug release is synthesized and named to be PDMC. Consequently, a multifunctional biomimetic coating based on the copolymer is prepared via a facile and flexible polydopamine (PDA) mediated layer-by-layer (LBL) self-assembly method for simultaneously achieving effective lubrication, bacteriostatic, and bactericidal performances, as shown in Scheme 1. The titanium alloy (Ti6Al4V) is chosen as a typical biomedical implant substrate, and the PDA acts as an anchoring and intercalated agent to facilitate the self-assembly process of the multilayered coating.[24] It is hypothesized that the multifunctional biomimetic coating developed herein can not only effectively enhance lubrication and bacteriostatic property based on the tenacious hydration shell, but also achieve excellent bactericidal performance depending on the CDs containing antibiotics. In the present study, the lubrication, drug loading and release, biocompatibility, and bacteriostatic/bactericidal properties of the coating are

investigated, and it preliminarily proves that the multi-functional biomimetic coating may be potentially applied for surface functionalization of biomedical implants.

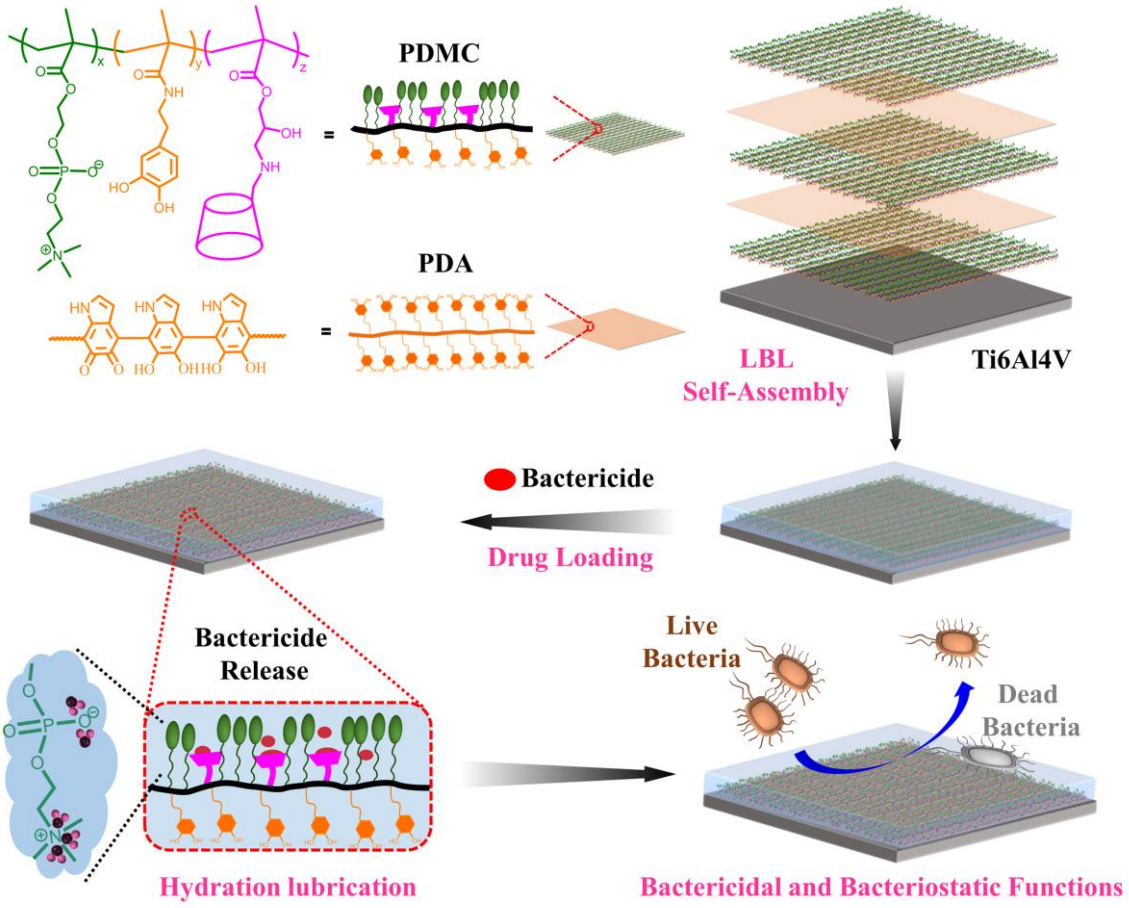

Scheme 1. Schematic illustration showing surface functionalization of Ti6Al4V using PDMC copolymer for lubrication enhancement and antibacterial performance.

2 Results and discussion

Copolymer Synthesis and Characterization

To incorporate the self-adhesion, lubrication, and drug loading & release properties into one system, the PDMC copolymer containing DMA, MPC, and CD is developed in this work. The copolymer is synthesized by free radical polymerization of DMA, MPC, and 3-(6-amino-β-CD)-2-hydroxypropyl methacrylate (MA-β-CD) using azodiisobutyronitrile (AIBN) as an initiator, as shown in Figure 1a. The 1H NMR

spectrum is used to confirm the successful preparation of the PDMC copolymer, and the result is provided in Figure 1b. The synthesis procedure and 1H NMR spectra of DMA and MA-β-CD are demonstrated in Figures S1 and S2, Supporting Information. The characteristic signals of DMA, MPC, and CD units are observed, and all the peaks are well assigned with their chemical structures. The signals at 2.83, 3.75, 3.99, 4.26, and 5.01 ppm are assigned to the protons of MA-β-CD, while the signals at 3.16, 3.35, and 4.26 ppm are attributed to the protons of MPC. The inclusion of DMA in the copolymer is confirmed by the proton peaks of dopamine moieties (δ = 2.68, 2.90, and 6.82 ppm). It is noted that the content of DMA (5%) and MA-β-CD (10%) in the copolymer is smaller than that in the feed ratio (both are 16%), indicating that DMA and MA-β-CD monomers are less reactive in the polymerization reaction than MPC monomer.

The weight-average molecular weight (Mw) of the PDMC copolymer is measured by GPC (retention time: 7.8 min), and the corresponding chromatogram is demonstrated in Figure 1c. From the GPC analysis using the standard polystyrene sample, the Mw of the copolymer is determined to be 175.8 kDa with a polydispersity (PDI) of 4.2. Since the molecular weight of the copolymer is large enough, it is expected that the copolymer can be stably modified on the Ti6Al4V substrate and other implant surfaces.[25] Overall, the results of 1H NMR and GPC analysis confirm the successful synthesis of the PDMC copolymer.

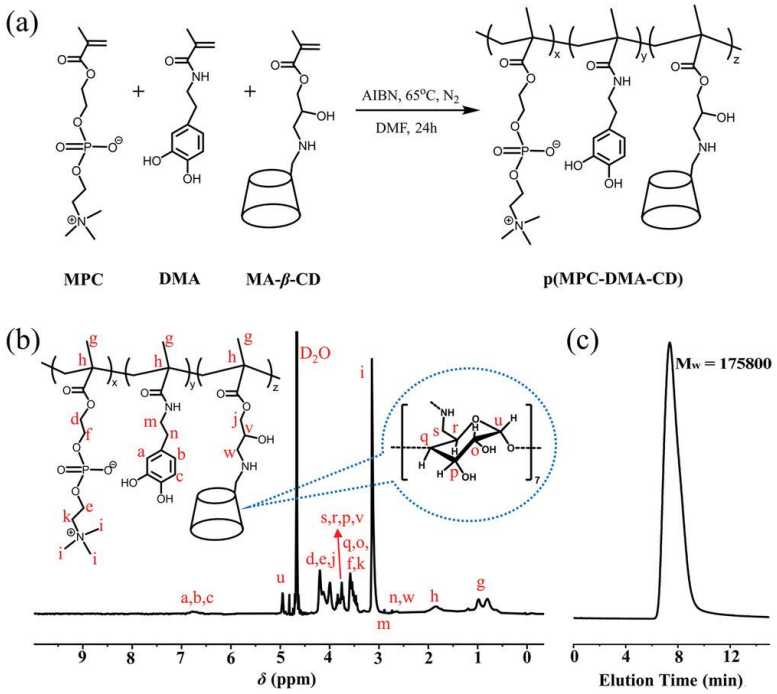

Figure 1. Synthesis and characterization of PDMC copolymer. a) Synthesis route; b) 1H NMR spectrum; c) GPC chromatogram.

Copolymer Self-Assembly on Ti6Al4V Substrate

To obtain a robust coating for achieving lubrication and bacterial resistance, a dopamine deposition technique is used to fabricate the PDMC-based self-adhesive coating on the Ti6Al4V substrate by the LBL method. Generally, dopamine can form a PDA coating layer that strongly adheres on the substrates through the interactions of covalent bond and noncovalent bond between various heterogeneous derivatives.[26, 27] The structure of DMA segment in the PDMC copolymer is quite similar to that of dopamine, and it can interact with PDA and adsorb onto the Ti6Al4V surface via multiple intermolecular interactions.[28] In the preparation of dopamine-based functional coating, the cation-π interaction is considered to be the primary mechanism for intermolecular self-assembly. Regarding the PDMC-based LBL coating in this study, the intermolecular interactions in PDA and PDMC and those interactions, which exist

between PDA and PDMC, can effectively facilitate and mediate the self-adhesive coating process.

The QCM-D with dissipation monitoring is employed to characterize the self-adhesive performance of the coating. Figure 2a shows the QCM-D data in terms of the measured changes in the oscillation frequency (Δf) and dissipation factor (ΔD) in the fabricating process of the PDMC-based LBL coating. The Δf represents the adsorbed mass and ΔD indicates the soft or rigid state of the adsorbed layer. Generally, a high value of ΔD/Δf indicates that the formed layer is relatively soft, while a low value of ΔD/Δf indicates a rigid adsorption.[29] If ΔD/(−Δf/n) is smaller than 4 × 10−7 for a 5 MHz crystal, then the film can be approximated as rigid, and the Sauerbrey equation can be used to extract the thickness of the film.[30] Here, deionized water and Tris-HCl are used to generate the baseline and remove the weakly adsorbed materials on the substrate. The LBL self-assembly of PDMC and PDA follows the steps below, PDMC → PDA → PDMC → PDA → PDMC. The final changes in Δf (−203 Hz) and ΔD (3.8 × 10−6) of the actual deposition of the PDMC and PDA coating indicate that the coating can be regarded as a rigid film. In Figure 2b, the overtone trends for Δf/n and ΔD/n (n = 3, 5, 7, 9, and 11) further indicate that the presence of the deionized water results in a rigid film with no significant differences among overtones in either frequency or dissipation. It is different from the function of Tris-HCl, which contributes to a viscoelastic film with additional energy dissipation and frequency (overtone)-dependent responses. Consequently, based on the Sauerbrey equation, the thickness of the LBL coating is calculated as about 36.0 nm. The thickness of the LBL coating (at dry condition) is also measured based on the

ion beam stripping method by XPS, and the result shown in Figure S3, Supporting Information, indicates that the thickness is about 25.0 nm, which is smaller than that obtained by QCM-D. Figure 2c shows the analysis of the ΔD/Δf absolute value in the adsorption process of PDMC and PDA. The ΔD/Δf absolute values of PDMC (about 0.09, 0.08, and 0.07) are all slightly higher compared with that of PDA (about 0.07 and 0.06). These data indicate that the PDMC adsorption onto the substrate is slightly softer than PDA, with more hydrated water in the moiety.[31] In addition, when the PDA is pumped across the sensor surface, it first removes the weakly adsorbed PDMC causing a decrease in Δf and ΔD, and then the PDA adsorbed mass increases with a decrease in ΔD, as shown in Figure 2d. Therefore, it is obvious that PDA can not only act as an anchoring and intercalated agent, but also adjust the viscoelasticity of the LBL coating.

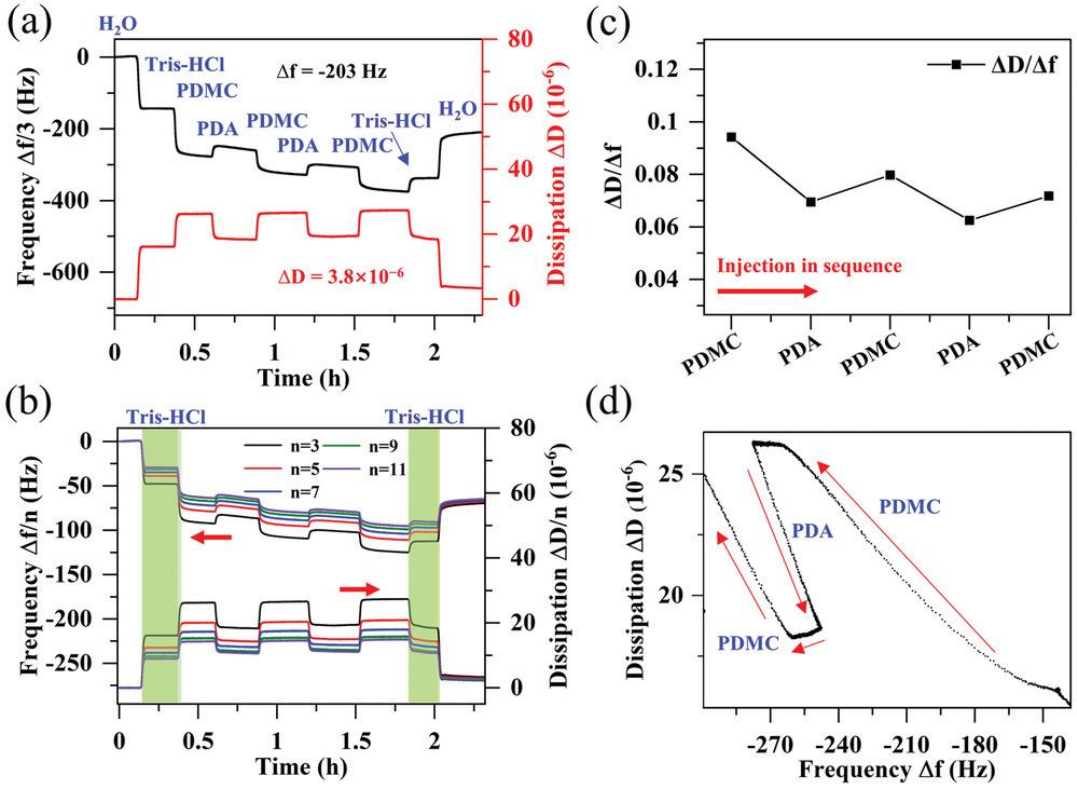

Figure 2. The self-adhesive performance of the LBL coating. a) Changes in frequency Δf and dissipation ΔD associated with the PMDC and PDA; b) Overtone trend for

Δf/n and ΔD/n; c) ΔD/Δf absolute value of PDMC and PDA in the adsorption process; d) ΔD versus Δf curve of PDMC and PDA in the adsorption process.

The XPS spectra are employed to examine the surface chemistry of different Ti6Al4V substrates, as exhibited in Figure 3a. The peaks of C 1s (285 eV), O 1s (530 eV), Ti 2p (458 eV), and Ti 3p (37 eV) are shown in bare Ti6Al4V. Regarding Ti6Al4V@PDMC, in addition to C1s, O1s, Ti 2p, and Ti 3p core level signals, new peaks with the binding energy at 402 and 133 eV are attributed to N 1s and P 2p core level signals, which correspond to the N+(CH3)3 and PO4− groups of MPC units in the PDMC copolymer.[32] In addition, the signal of Ti 3p also decreases after modification with the PDMC-based LBL coating. The result indicates that the PDMC-based LBL coating has been successfully fabricated onto the Ti6Al4V substrate. Furthermore, the high-resolution narrow spectrum of N 1s as shown in Figure 3b is deconvoluted into three types, which correspond to the amide, secondary amine, and quaternary ammonium groups (i.e., 398 eV for □NHCO□ group of DMA, 399 eV for □NH□ group of MA-β-CD, and 402 eV for □N+(CH3)3 group of MPC) in the copolymer, respectively. Meanwhile, the high-resolution narrow spectrum of P 2p shows that the peak at 133 eV corresponds to the PO4− group, which is consistent with previously reported studies (Figure 3c).[15, 16]

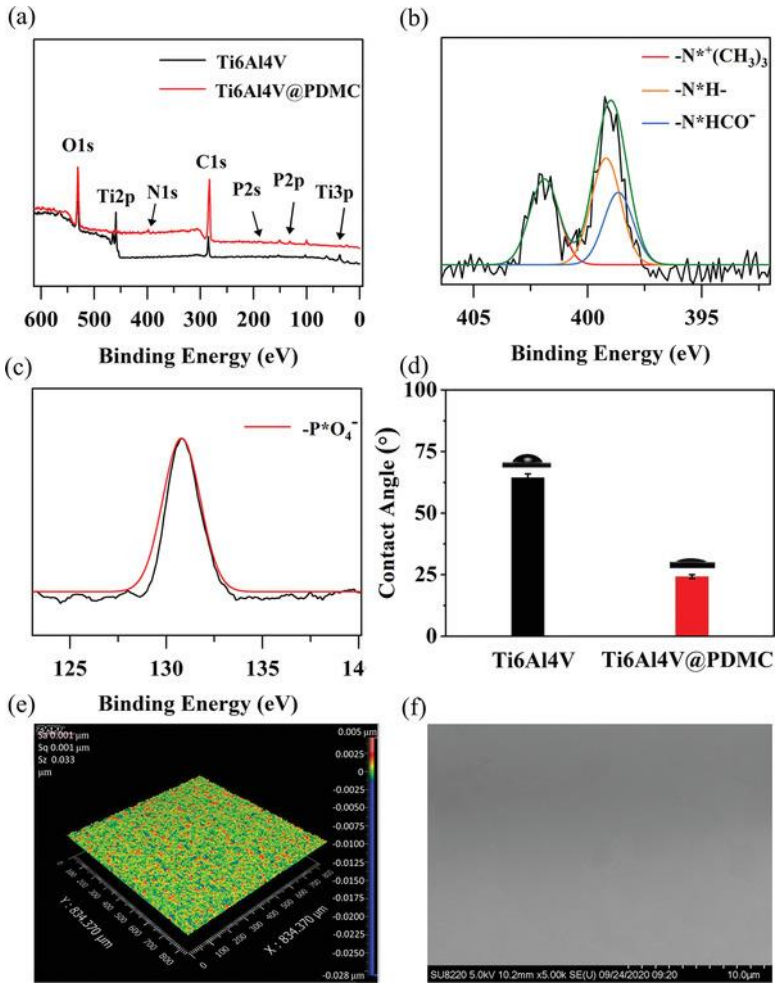

Figure 3. Surface characterizations of copolymer-modified Ti6Al4V substrate. a) XPS analysis of bare Ti6Al4V and Ti6Al4V@PDMC. b,c) High-resolution narrow spectra of N 1s and P 2p of Ti6Al4V@PDMC. d) Water contact angle of bare Ti6Al4V and Ti6Al4V@PDMC. The data are shown as mean value ± standard deviation. e,f) Surface topography/morphology of Ti6Al4V@PDMC examined using an optical interferometer and an SEM.

Wettability is an essential component in the design and development of biocompatible surfaces. The water contact angle analysis is used to investigate the interfacial wetting behavior of the PDMC copolymer that is coated onto the surface of Ti6Al4V substrate. As shown in Figure 3d, the water contact angle of bare Ti6Al4V (64.5 ± 1.5°) is much higher than that of Ti6Al4V@PDMC (24.3 ± 0.8°), which indicates that the copolymer

coating has greatly enhanced the surface hydrophilicity of Ti6Al4V substrate. It is considered that the MPC units within the PDMC copolymer, which can interact with water molecules via hydrogen bonding and correspondingly induce the formation of a hydration layer surrounding the zwitterionic charges, significantly improve the hydrophilicity. Besides, the CD groups in the copolymer also contribute to the increased hydrophilicity of Ti6Al4V substrate.

Surface roughness is another factor that can affect the surface wettability. Basically, the Wenzel and Cassie model can be used to describe the relationship between the surface roughness and the wettability of a surface.[33, 34] Through the characterization of surface topography for bare Ti6Al4V (Figure S4a, Supporting Information) and Ti6Al4V@PDMC (Figure 3e), the surface roughness values (Sa) of the bare Ti6Al4V and copolymer-coated Ti6Al4V samples are both about 1 nm. This result conforms to the surface morphology of bare Ti6Al4V (Figure S4b, Supporting Information) and Ti6Al4V@PDMC (Figure 3f), which indicates that the surfaces are very smooth and the LBL coating is uniformly prepared on the substrate. Therefore, it is considered that the effect of surface roughness on wettability can be ignored, and the increased hydrophilicity of Ti6Al4V@PDMC is attributed to the phosphorylcholine groups with zwitterionic charges and also the CD moieties with hydroxyl groups.

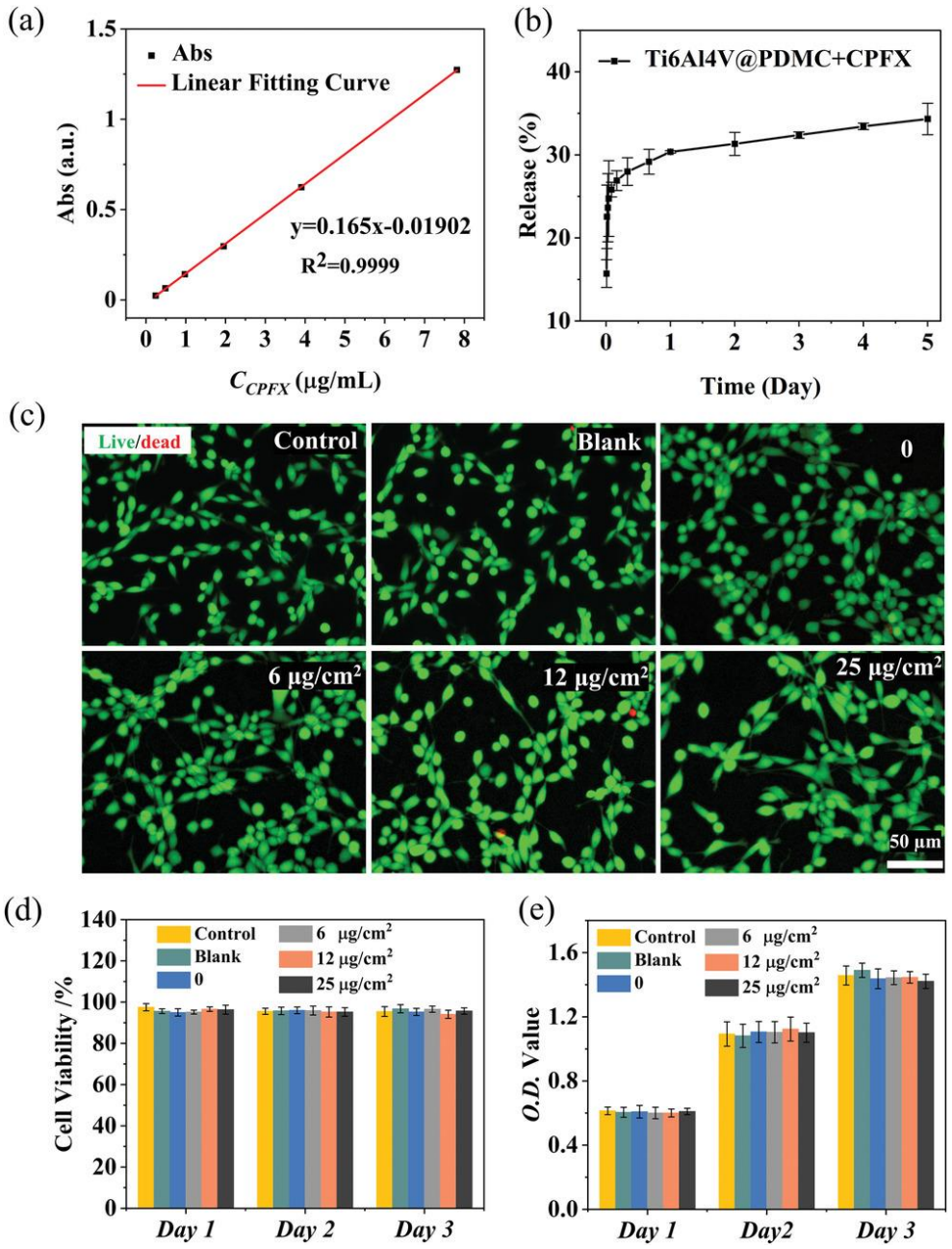

Figure 4. The drug release and biocompatibility property of Ti6Al4V@PDMC+CPFX samples. a) Standard curve of CPFX in deionized water. b) Release profile of CPFX from Ti6Al4V@PDMC+CPFX. c) Live/Dead staining of L929 cells cultured with the control, blank (bare Ti6Al4V), and Ti6Al4V@PDMC with 0, 6, 12, and 25 μg cm−2 of CPFX. d) Cell viability and e) Cell proliferation results of L929 cells after culturing for 1, 2, and 3 days with the control, blank (bare Ti6Al4V) and Ti6Al4V@PDMC with 0,

6, 12, and 25 μg cm−2 of CPFX, respectively. The data are shown as mean value ± standard deviation.

Drug Loading and Release.

Ciprofloxacin hydrochloride (CPFX) is chosen as the model cargo for the drug loading and release test. According to the standard curve of CPFX, as shown in Figure 4a, the amount of CPFX encapsulated into the Ti6Al4V@PDMC sample (in 0.5 mg mL−1 CPFX solution) is 25 μg cm−2. Figure 4b displays the in vitro cumulative drug release of CPFX from the PDMC-based LBL coating at 37 °C, which shows typically two different stages. The typical drug release profile is characterized by an initial burst release phase and then followed by a slow-release phase. The initial burst release phase is observed from 0.15 to 16 h, which is mainly attributed to desorption of the surface-adsorbed drug by electrostatic interactions.[35] The following sustained release phase starts from 16 h and continues up to 5 days, and it corresponds to the release of CPFX which has been pre-loaded into the CD groups of the copolymer. In addition, the release of CPFX from the PDA and p(DMA-MPC) coatings as control groups are investigated, and the results are shown in Figure S5, Supporting Information. The amount of CPFX encapsulated into the Ti6Al4V@PDA and Ti6Al4V@DMA-MPC samples is 4.3 and 2.86 μg cm−2, and the cumulative drug release after 24 h is approximately 85% for Ti6Al4V@PDA and 90% for Ti6Al4V@DMA-MPC. Overall, the result of in vitro drug release test indicates that the release of CPFX from the PDMC-based LBL coating is endowed with a sustained release behavior, which is beneficial for achieving long-term antibacterial performance.

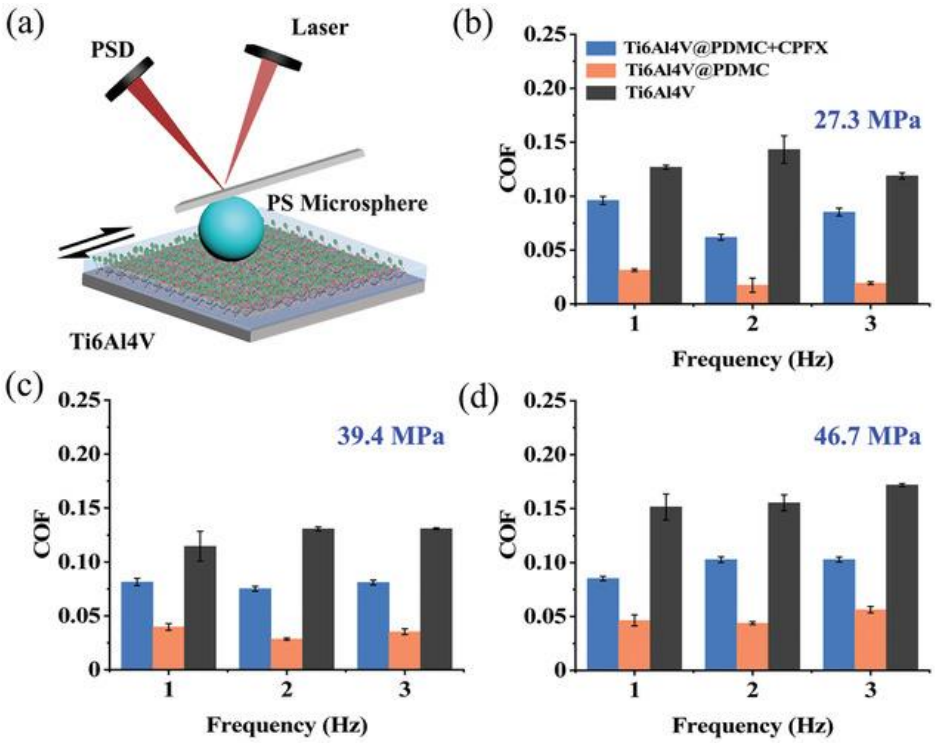

Figure 5. The lubrication property of various copolymer-coated Ti6Al4V substrates. a) Schematic diagram showing the experimental setup of the lubrication test. b–d) COF-frequency plots for PS microsphere contacted with bare Ti6Al4V, Ti6Al4V@PDMC, and Ti6Al4V@PDMC+CPFX (25 μg cm−2) under different pressures of b) 27.3 MPa, c) 39.4 MPa, and d) 46.7 MPa, respectively. The data are shown as mean value ± standard deviation.

Biocompatibility

The biocompatibility of the Ti6Al4V@PDMC and Ti6Al4V@PDMC+CPFX samples with different amounts of pre-loaded drug is evaluated using the L929 cells according to the ISO 10993 standard, and the results are as shown in Figure 4c–e. It is clear that very few dead cells are present for all the samples in each group, and the cell viability is over 90% from day 1 to day 3. In addition, the L929 cells in each group can proliferate well during the whole incubation time with no significant differences among different groups. These results indicate that all the samples including the drug-loaded (6, 12, and

25 μg cm−2 of CPFX) Ti6Al4V@PDMC sheets show satisfied biocompatibility and will not induce potential adverse effects to the nearby tissues after implantation.

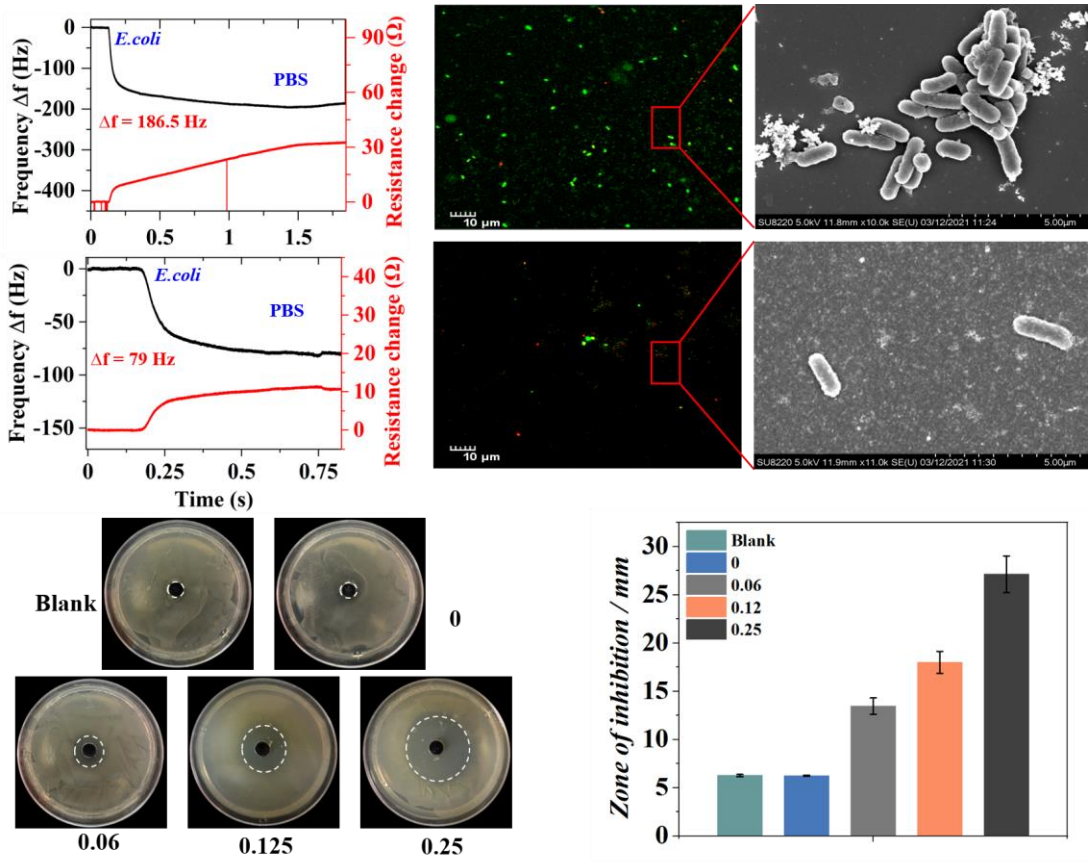

Figure 6. The antibacterial activity properties of biomimetic self-adhesive coating. a,b) Frequency and resistance changes associated with dynamic adsorption of E. coli on the surface of a) bare and b) copolymer-coated Au□Ti sensors. c,d) Confocal microscopic images of c) bare and d) copolymer-coated Au□Ti sensors after dynamic adsorption of E. coli by QCM. The bacteria are stained with Live/Dead BacLight bacterial viability kit. Live bacteria with intact membranes display green fluorescence, while those with damaged membranes show red fluorescence. e,f) Typical SEM images exhibiting morphological changes of E. coli membrane in contact with e) bare and f) copolymer-coated Au□Ti sensors. g,h) Inhibition zones of the samples in blank (bare Ti6Al4V) and Ti6Al4V@PDMC groups containing 0, 6, 12, and 25 μg cm−2 of CPFX against E. coli. The data are shown as mean value ± standard deviation.

Lubrication Property

The low surface roughness and excellent surface wettability indicate that the Ti6Al4V substrate has been successfully coated with the PDMC copolymer onto the surface. The further investigation—lubrication property—of the self-assembly coating is performed by measuring the friction forces under a series of applied normal pressures in phosphate-buffered solution (PBS). The schematic setup of the tribological test is displayed in Figure 5a with a typical contact tribopair between the polystyrene (PS) microsphere and Ti6Al4V sheet (bare, copolymer-coated, and copolymer-coated and drug-loaded), and Figure 5b–d presents the COF versus frequency plots under different pressures of 27.3, 39.4, and 46.7 MPa. Clearly, the COF values of Ti6Al4V@PDMC are lower than that of bare Ti6Al4V and Ti6Al4V@PDMC+CPFX. For example, the COF value decreases remarkably from 0.152 for bare Ti6Al4V to 0.042 for Ti6Al4V@PDMC at 46.7 MPa (1 Hz). The COF value of Ti6Al4V@PDMC+CPFX is still lower than that of bare Ti6Al4V under all test conditions. It is considered that the increased COF value of Ti6Al4V@PDMC+CPFX in comparison with Ti6Al4V@PDMC is related to its relatively lower hydrophilicity, where the water contact angle is measured to be about 42.9 ± 2.3°, as shown in Figure S6, Supporting Information. The durability of the copolymer coating is shown from the relatively stable COF value of Ti6Al4V@PDMC under different frequencies and pressures. Such excellent resistance to high pressure is attributed to the formation of a tenacious hydration shell surrounding the MPC segment of the PDMC copolymer coating in aqueous media, where the hydration layer induces a significant improvement in lubrication with a fluidlike response to shear between two sliding surfaces.

Antibacterial Activity

It is reported that the phosphorylcholine groups in the PDMC copolymer can adsorb a large quantities of water molecules surrounding the zwitterionic charges, and thus form a tenacious hydration shell to effectively resist bacterial adhesion.[16] In order to further quantitatively evaluate the antibacterial performance of the biomimetic coating, QCM was applied to characterize the dynamic adsorption behavior of Escherichia coli (E. coli) on both bare and copolymer-coated Au□Ti sensors. In Figure 6a,b, it is obvious that the absolute value of Δf (79 Hz) for the copolymer-coated Au□Ti sensor is significantly smaller than that of bare sensor (186.5 Hz), indicating that the PDMC-based LBL coating has a reduced bacterial adsorption. According to Sauerbrey equation, the Sauerbrey mass of E. coli adsorption on the surface of copolymer-coated Au-Ti sensor is 28.44 ng cm−2, while that on the uncoated bare sensor is 67.14 ng cm−2. Therefore, the bacterial resistance ratio of Ti6Al4V@PDMC is calculated as more than 58%, achieving good bacterial resistance performance.

The bacterial strain of E. coli is used for evaluating the capability of copolymer-coated substrate to inhibit bacterial adhesion by the Live/Dead two-color fluorescence method. As demonstrated in Figure 6c,d, the bacterial distribution on the surface of bare and copolymer-coated Au□Ti sensors is observed by being stained with a combination dye of SYTO9 and PI. Numerous readily distinguishable bacterial cells are distributed on the bare Au□Ti sensor surface with green fluorescence after the quantitative evaluation of dynamic adsorption of E. coli by QCM. However, only several single bacterial cells can be detected on the copolymer-coated Au□Ti sensor surface. Obviously, the number

of E. coli adhered on the Ti6Al4V@PDMC surface is less than that on the bare Ti6Al4V surface, which is consistent with the result of QCM test. Additionally, the SEM analysis of E. coli after the dynamic adsorption by QCM further reveals no significant changes in surface morphology upon interaction with the PDMC-based LBL coating, and most of the bacterial cells are viable on the surface with the intact cell membrane (as shown in Figure 6e,f). The above results indicate that the PDMC-based LBL coating modified on the Ti6Al4V substrate induces excellent bacterial resistance performance but with no antimicrobial effect.

Furthermore, to validate the antimicrobial effect of the loaded CPFX in the biomimetic coating, the inhibition zone test is performed with E. coli, and the results are shown in Figure 6g,h. It is clear that the samples in the blank and 0 (no CPFX) groups present no obvious inhibition zones. However, after incorporation of CPFX in the coating, the inhibition zone against E. coli can be observed for the samples. Moreover, the inhibition zone becomes larger with the increase in the amount of loaded CPFX. Quantitatively, the inhibition zone for the 25 μg cm−2 group shows 1.5-folds and 2-folds larger compared with that of the 12 and 6 μg cm−2 groups.

3. Conclusions

In the present study, a bioinspired surface functionalization strategy was developed for achieving enhanced lubrication and synergistic bacteriostatic/bactericidal performance, using a newly synthesized PDMC copolymer by free radical polymerization. Ti6Al4V was utilized as a typical material for biomedical implant, and various characterizations confirmed that the copolymer was successfully coated on the Ti6Al4V substrate based

on an LBL self-assembly method with a thickness of around 36 nm. The tribological test and bacterial resistance test revealed that the lubrication enhancement and antibacterial adhesion property of Ti6Al4V@PDMC was due to the tenacious hydration shell formed surrounding the zwitterionic charges within the copolymer. Additionally, the prolonged bactericidal function of the biomimetic coating was further achieved after pre-loading bactericide into the CD cavities for sustained drug release, which could kill the bacteria adhered to the substrate. In conclusion, the bioinspired polymeric coating developed in this study may be used as an effective surface functionalization strategy to achieve both enhanced lubrication and synergistic bacteriostatic/bactericidal property for biomedical implants.

4. Experimental Section

Materials and Methods.

Dopamine hydrochloride, methacrylic anhydride, glycidyl methacrylate (GMA), and mono-(6-deoxy-6-amino)-β-cyclodextrin (6-amino-β-CD) were purchased from J&K Scientific Ltd., Beijing, China. Sodium tetraborate (NaB_4O_7), sodium bicarbonate ($NaHCO_3$), Tris-HCl buffer, CPFX, PS microspheres, and AIBN were purchased from Aladdin Bio-Chem Technology Co., Ltd., Shanghai, China. High-purity Ti6Al4V sheet was purchased from Goodfellow Cambridge Ltd., Huntingdon, UK. Live/Dead BacLight Bacterial Viability Kit was purchased from Thermo Fisher Scientific (China) Ltd., Shanghai, China. MPC was purchased from Joy-Nature Institute of Technology, Nanjing, China.

Synthesis of p(DMA−MPC−CD) copolymer.

DMA was prepared based on the procedure reported in the previous study,[16] and MA-β-CD was synthesized according to the route provided in one previous study.[36] The p(DMA-MPC-CD) copolymer was synthesized by free-radical copolymerization of DMA, MPC, and MA-β-CD at a feeding mole ratio of 1:1:4 using AIBN as an initiator. Briefly, DMA (0.150 g), MPC (0.529 g), MA-β-CD (0.300 g), and AIBN (3 mg) were dissolved in 50 mL of N,N-dimethylformamide under nitrogen atmosphere, and the reaction was proceeded at 65 °C for 24 h. Subsequently, the solution was dialyzed against deionized water and freeze-dried to obtain a flocculent product. The p(DMA-MPC-CD) copolymer was named PDMC for short.

LBL Self-Assembly Coating on Ti6Al4V Substrate

The bare Ti6Al4V sheet (size: 10 mm × 10 mm × 1 mm) was chemically mechanically polished by using a 90% colloidal silica suspension and 10% H2O2 solution, and ultrasonically cleaned in deionized water for 10 min. The PDMC copolymer solution (5 mg mL−1) was prepared through dissolving the copolymer in Tris-HCl solution (pH = 8.5). The surface modification process of the copolymer on Ti6Al4V substrate was described as follows. The Ti6Al4V substrate was immersed in the PDMC copolymer solution and remained for 24 h in the dark, rinsed with 100 mL of deionized water three times, and finally dried in air. Subsequently, the PDMC-modified substrate was immersed in 1 mg mL−1 of dopamine solution (dissolved in Tris-HCl solution, pH = 8.5) and remained for 24 h, which was followed by the same rinsing and drying steps as mentioned above. The following PDMC, PDA, and PDMC coatings were fabricated consecutively in the same way as previously described. Finally, the Ti6Al4V substrate

with LBL self-assembly coating, namely, Ti6Al4V@PDMC, was sufficiently rinsed with deionized water and dried under vacuum.

Characterizations of PDMC Copolymer and PDMC-Modified Ti6Al4V Substrate

The 1H nuclear magnetic resonance (1H NMR) spectra of DMA, MA-β-CD, and PDMC were obtained by an NMR spectrometer (AVANCEIII, Bruker, Germany) with dimethyl sulfoxide (DMSO-d6) and deuterium oxide (D2O) as the solvents. The weight-average molecular weight (Mw) distribution of PDMC was analyzed utilizing a gel permeation chromatography system (GPC, Viscotek TDA305max, Malvern Instruments, UK) with sodium nitrate to be the diluent (0.1 M, flow rate: 0.7 mL min−1). The surface elemental compositions of Ti6Al4V and Ti6Al4V@PDMC were characterized employing an X-ray photoelectron spectroscopy spectrometer (XPS, PHI Quantera II, Bruker, Billerica, USA) equipped with a 15 kV Mg Kα radiation source. The static water contact angle of Ti6Al4V and Ti6Al4V@PDMC was measured by a goniometer (OCA-20, Dataphysics Instruments, Filderstadt, Germany) based on the sessile drop method. The pipette was used to place a drop of ultrapure distilled water (approximately 4 μL) on the surface of the samples each time. The measurement was repeated for at least three times for each sample, and the average value was calculated. The surface morphology and topography of Ti6Al4V and Ti6Al4V@PDMC was evaluated using a scanning electron microscope (SEM, SU8220, Hitachi, Japan) and an optical interferometer (NexView, ZYGO, USA), respectively.

The thickness of LBL self-assembly coating on the Ti6Al4V substrate was analyzed employing a quartz crystal microbalance (QCM-D, Q Sense Explorer, Biolin Scientific,

Sweden). The measurement was carried out on a Ti-coated quartz crystal (Au□Ti sensor), which was prepared by sputter coating of a thin Ti layer on the surface of quartz crystal (JS-3, Institute of microelectronics of the Chinese Academy of science, China). The Au□Ti sensor was placed into the flow chamber, and deionized water and Tris-HCl solution (pH = 8.5) were pumped over the sensor surface in sequence and stabilized for 10 min to generate the baseline. Subsequently, PDMC copolymer in Tris-HCl buffer (5 mg mL−1, pH = 8.5) was pumped into the flow chamber for 15 min, which was followed by the dopamine solution (in Tris-HCl buffer, 1 mg L−1, pH = 8.5) for 15 min. The above PDMC copolymer and dopamine solutions were pumped into the flow chamber consecutively for 15 min to achieve the LBL self-assembly coating process. Finally, Tris-HCl buffer (pH = 8.5) and deionized water were pumped over the sensor surface in sequence and stabilized for 10 min, respectively. The flow rate of the solutions used for all the steps was 100 μL/min, and the temperature was 25 °C. The changes in thickness (Δδ) of the quartz crystal sensor were calculated according to the Sauerbrey equation[37] as shown below, where Δf was the resonant frequency shift of the sensor, and n represented the overtone number (n = 3 in this work, unless otherwise specified). Additionally, the thickness of LBL self-assembly coating on the Ti6Al4V substrate at dry condition was measured based on the ion beam stripping method by XPS, from which the intensity of the C and N elements were recorded with different etching depth of the sample:

$$\Delta\delta = 17.7 * \frac{\Delta f}{100n}(nm)$$

where Δf was the resonant frequency shift of the sensor, *n* represented the overtone

number (n = 3 in this work).

In vitro drug loading and release test

he Ti6Al4V@PDMC samples (n = 5) were added to 2 mL of CPFX solution (0.5 mg mL−1 in deionized water). After 24 h, the CPFX-loaded sheets (namely, Ti6Al4V@PDMC+CPFX) were washed with deionized water three times, and dried under vacuum. The amount of CPFX remaining in the solution was analyzed by a UV–vis spectrophotometer (UV-6100s, Metash Instruments, China) at a wavelength of 277 nm. Three parallel replicates were performed for repeatability. The relationship between CPFX concentration in deionized water and its absorbance at the wavelength of 277 nm was measured beforehand as the reference. The total loading dosage of CPFX was calculated by subtraction of the total solute in the initial solution and the remaining solution. Subsequently, the Ti6Al4V@PDMC+CPFX samples were placed into 2 mL of deionized water for a drug release test. The drug release percentage (wt %) was calculated based on the following Equation. Finally, the cumulative release-time curve of CPFX was plotted. All the independent tests were repeated at least three times to verify the result, and the data were presented as mean ± standard deviation. The drug loading and release tests of the Ti6Al4V@PDA and Ti6Al4V@DMA-MPC samples were also performed based on a similar method as mentioned above, and the procedures for preparing the Ti6Al4V@PDA and Ti6Al4V@DMA-MPC samples were provided in the Supporting Information.

$$drug\ \ release\ \ percentage(\%) = \frac{\text{amount of released CPFX}}{\text{total amount of loaded CPFX}} \times 100$$

Biocompatibility Evaluation

The Ti6Al4V@PDMC samples with different amounts of pre-loaded CPFX were prepared by immersing the sheets (n = 20) into 2 mL of CPFX solution (17, 35, and 70 μg mL−1 in deionized water, respectively). After 24 h, the CPFX-loaded Ti6Al4V@PDMC were washed with deionized water three times, and finally dried under vacuum. The biocompatibility of the prepared samples was characterized according to the ISO 10993 standard. Briefly, L929 cells were seeded in a 24 well plate at a density of 6 × 104 cells per well and cultured in Dulbecco's Modified Eagle's Medium (DMEM, Gibco, China) supplemented with 10% fetal bovine serum (Gibco, China) and 1% penicillin/streptomycin (Gibco, China) at 37 °C and 5% CO2. Afterwards, the sterile samples were added to the 24-well plate for biocompatibility investigation. Briefly, the pure medium group and bare Ti6Al4V sheet were used as control and blank groups. On days 1, 2, and 3, the Live/Dead assay (Thermo Fisher, China) was performed to evaluate cell viability according to the manufacturer's instructions, which was quantified by the ratio between the live cells and the total cells. In addition, the MTT assay was used to quantify cell proliferation. The absorption at a wavelength of 570 nm indicating the cell metabolic activity was recorded by a plate reader (BioTek, USA).

Lubrication Experiment

A series of tribological tests were performed to evaluate the lubrication property of the PDMC copolymer using an atomic force microscope (AFM, MFP-3D, Asylum Research, Santa Barbara, USA) in contact mode. Briefly, aminated PS microsphere (diameter ≈ 5 μm) was glued on the jut of a rectangular tipless silicon cantilever (“TL-

CONT" type, NanoWorld AG, Neuchatel, Switzerland) through ultraviolet irradiation for 40 min. The spring constant of the cantilever was calibrated by the frequency method,[38] and the lateral sensitivity of the cantilever was determined using the improved wedge calibration method.[39] The COF values between the PS microsphere and the Ti6Al4V sample (bare or copolymer-coated) in PBS were collected at room temperature under various loads from 50 to 250 nN (equivalent to the maximum contact pressure of 27.3 (50 nN), 39.4 (150 nN), and 46.7 MPa (250 nN), respectively),[40] various scan rates from 1 to 3 Hz, and a sliding distance of 20 μm. Three rectangular areas (20 μm × 20 μm) were randomly scanned in the same test condition. The average COF value and standard deviation were calculated from three data points, and each data point was obtained from a total of 256 scans across the rectangular area.

Bacterial Resistance Performance

A QCM (QCM922A, SEIKO EG&G, Japan) was utilized to quantitatively evaluate the dynamic adsorption of E. coli (E. coli, ATCC8739) on the copolymer-coated substrate. E. coli was incubated in Luria-Bertani (LB, Sigma-Aldrich, USA) medium overnight, and the bacterial suspension was diluted to a concentration of approximately 1 × 108 cfu mL−1. The Au-Ti sensors with or without the PDMC copolymer coating were placed into the flow chamber, and air and PBS were pumped over the sensor surface in sequence to generate the baseline. Then the E. coli solution was pumped into the chamber at a flow rate of 200 μL min−1 at 25 °C, which was followed by the rinsing of PBS until the measurement was stable. Specifically, Δf and Δm/A presented a linear relationship, which could be described within the context of the Sauerbrey theory.[41,

42] In this equation, fn was the overtone frequency of the QCM (fn = nf0; n = 3; f0 = fundamental oscillation frequency), A was the electrode area (0.196 cm2), and ρc and μc were the quartz density (2.65 g cm−3) and shear modulus (2.947 × 1011 g (cm s2)−1, respectively. According to this equation, a frequency change of 1 Hz corresponded to a mass density increase of 0.36 ng cm−2 for the 8.95 MHz QCM used in this study.

$$\Delta \mathrm{f} = -\frac{2(\mathrm{f}_n)^2}{\sqrt{\rho_c \times \mu_c}} \frac{\Delta \mathrm{m}}{A} (Hz)$$

The bacterial resistance of the PDMC terpolymer coating was calculated based on the following equation, where MTi6Al4V represented the bacterial mass of the uncoated group, and MTi6Al4V@PDMC represented the bacterial mass of the coated group.

$$bacterial\ resistance\ ratio\ (\%) = (M_{\mathrm{Ti6Al4V}} - M_{\ \mathrm{Ti6Al4V@PDMC}})/M_{\mathrm{Ti6Al4V}} \times 100$$

After the quantitative evaluation of dynamic adsorption of E. coli by QCM, the Au□Ti sensor was stained by propidium iodide (PI) and SYTO9 according to the instructions of the manufacturer. After being stained for 10 min in the dark, the excess stains were washed off, and the bacteria on the samples were observed by a confocal laser scanning microscope (CLSM, FV 3000RS, OLYMPUS, FluoView, Japan). Additionally, the morphological changes of the bacteria upon contact with the PDMC-based LBL coating were examined by SEM. In brief, the samples were placed in 2.5% glutaraldehyde/PBS solution at 4 °C overnight. After fixation, these samples were washed thrice with sterile PBS, and sequentially dehydrated using a graded series of ethanol solutions (20%, 40%, 60%, 80%, and 100%). Finally, the samples were sputter-coated with platinum and then

observed using the SEM.

Antimicrobial Capacity Test

The inhibition zone assay was performed to evaluate the antimicrobial activity of various sheets including bare Ti6Al4V, Ti6Al4V@PDMC, and Ti6Al4V@PDMC+CPFX (prepared as described above). Briefly, all the samples were sterilized with UV exposure for 2 h, and then E. coli was adopted for the inhibition zone test. The E. coli at a density of 1 × 108 cfu mL−1 was placed on LB agar plates and cultured at 37 °C for 24 h. Next, different samples with a diameter of 6 mm were placed in the center of the agar plates and kept for 24 h. The antimicrobial capacity of different samples was observed and quantified based on the diameter of the inhibition zone.

Statistical Analysis

The experimental data were presented as mean value ± standard deviation, which were obtained from repeated tests at least three times to verify the result unless otherwise mentioned.

5. Acknowledgements

H.W. and Y.Y. contributed equally to this work. This study was financially supported by National Natural Science Foundation of China (52022043, 82122002), Tsinghua University–Peking Union Medical College Hospital Initiative Scientific Research Program (20191080593), Precision Medicine Foundation, Tsinghua University, China (10001020120), Capital's Funds for Health Improvement and Research (2020-2Z-40810), Research Fund of State Key Laboratory of Tribology, Tsinghua University,

China (SKLT2022C18) and Shenzhen Basic Research Project, Shenzhen Science and Technology Innovation Committee (2021Szvup141).

Reference

1. T. Røn, K. P. Jacobsen and S. Lee, *J. Mech. Behav. Biomed. Mater.*, 2018, **84**, 12-21.
2. L. Han, L. Xiang, J. Zhang, J. Chen, J. Liu, B. Yan and H. Zeng, *Langmuir*, 2018, **34**, 11593-11601.
3. B. Wang, Q. Lin, T. Jin, C. Shen, J. Tang, Y. Han and H. Chen, *RSC Advances*, 2015, **5**, 3597-3604.
4. H. Wan, K. Ren, H. J. Kaper, P. K. Sharma, J. Colloid Interface Sci. 2021, 594, 435.
5. B. Winkeljann, K. Boettcher, B. N. Balzer, O. Lieleg, Adv. Mater. Interfaces 2017, 4, 1700186..
6. K. Ishihara, Polym. J. 2015, 47, 585
7. V. N. Lazarev, V. M. Govorun, Appl. Biochem. Microbiol. 2010, 46, 803.
8. I. Banerjee, R. C. Pangule, R. S. Kane, Adv. Mater. 2011, 23, 690.
9. L. Sánchez-González, M. Cháfer, A. Chiralt, C. González-Martínez, Carbohydr. Polym. 2010, 82, 277.
10. E. P. Ivanova, J. Hasan, H. K. Webb, V. K. Truong, G. S. Watson, J. A. Watson, V. A. Baulin, S. Pogodin, J. Y. Wang, M. J. Tobin, C. Löbbe, R. J. Crawford, Small 2012, 8, 2489.
11. G. S. Watson, D. W. Green, L. Schwarzkopf, X. Li, B. W. Cribb, S. Myhra, J. A. Watson, Acta Biomater. 2015, 21, 109.
12. J. J. F. Klein, Friction 2013, 1, 1.
13. J. Seror, L. Zhu, R. Goldberg, A. J. Day, J. Klein, Nat. Commun. 2015, 6, 6497.
14. S. Jahn, J. Seror, J. Klein, Annu. Rev. Biomed. Eng. 2016, 18, 235..
15. S. Liu, Q. Zhang, Y. Han, Y. Sun, Y. Zhang, H. Zhang, Langmuir 2019, 35, 13189.
16. S. Liu, Q. Zhang, Y. Han, Y. Sun, Y. Zhang, H. Zhang, Langmuir 2019, 35, 13189.
17. Q. Wei, X. Liu, Q. Yue, S. Ma, F. Zhou, Langmuir 2019, 35, 8068.
18. S. Renvert, C. Lindahl, H. Renvert, G. R. Persson, Clin. Oral Implants Res. 2008, 19, 342.
19. T. Chen, L. Zhao, Z. Wang, J. Zhao, Y. Li, H. Long, D. Yu, X. Wu, H. Yang, Biomacromolecules 2020, 21, 5213.
20. L. Huang, L. Zhang, S. Xiao, Y. Yang, F. Chen, P. Fan, Z. Zhao, M. Zhong, J. Yang, Chem. Eng. J. 2018, 333, 1.
21. B. L. Wang, T. W. Jin, Y. M. Han, C. H. Shen, Q. Li, Q. K. Lin, H. Chen, J. Mater. Chem. B 2015, 3, 5501.
22. Y. Liu, K. Ai, L. Lu, Chem. Rev. 2014, 114, 5057.
23. G. Tiwari, R. Tiwari, A. K. Rai, J. Pharm. BioAllied Sci. 2010, 2, 72.
24. L. Yang, L. Li, H. Wu, B. Zhang, R. Luo, Y. Wang, J. Controlled Release 2020, 321, 59.
25. J. K. Park, K. S. Kim, J. Yeom, H. S. Jung, S. K. Hahn, Macromol. Chem. Phys. 2012, 213, 2130.
26. S. Hong, Y. Wang, S. Y. Park, H. Lee, Sci. Adv. 2018, 4, eaat7457.
27. S. Hong, Y. S. Na, S. Choi, I. T. Song, W. Y. Kim, H. Lee, Adv. Funct. Mater. 2012, 22, 4711.
28. A. S. Mahadevi, G. N. Sastry, Chem. Rev. 2013, 113, 2100
29. N. J. Cho, C. W. Frank, B. Kasemo, F. Höök, Nat. Protoc. 2010, 5, 1096.
30. A. D. Easley, T. Ma, C. I. Eneh, J. Yun, R. M. Thakur, J. L. Lutkenhaus, J. Polym. Sci. 2022, 60, 1090.
31. A. K. Dutta, G. Belfort, Sens. Actuators, B 2009, 136, 60.
32. Y. Xu, M. Takai, K. Ishihara, Biomaterials 2009, 30, 4930.

33. X. Ou, Z. Lin, J. Li, Chem. Commun. 2018, 54, 5418.
34. S. Pan, M. Chen, L. Wu, ACS Appl. Mater. Interfaces 2020, 12, 5457.
35. N. Blanchemain, Y. Karrout, N. Tabary, C. Neut, M. Bria, J. Siepmann, H. F. Hildebrand, B. Martel, Acta Biomater. 2011, 7, 304.
36. N. Azizi, M. R. Saidi, Org. Lett. 2005, 7, 3649.
37. K. A. Marx, Biomacromolecules 2003, 4, 1099.
38. C. P. Green, H. Lioe, J. P. Cleveland, R. Proksch, P. Mulvaney, J. E. Sader, Rev. Sci. Instrum. 2004, 75, 1988.
39. M. Varenberg, I. Etsion, G. Halperin, Rev. Sci. Instrum. 2003, 74, 3362
40. Y. Wang, Y. Sun, Y. Gu, H. Zhang, Adv. Mater. Interfaces 2019, 6, 1970075.
41. W. Diyatmika, C. C. Yu, Y. Tanatsugu, M. Yasuzawa, J. P. Chu, Thin Solid Films 2019, 688, 137382.
42. H. Seto, M. Harada, H. Sakamoto, H. Nagaura, T. Murakami, I. Kimura, Y. Hirohashi, H. Shinto, Adv. Powder Technol. 2020, 31, 4129.